Molecular Therapy
Original Article

Recombinant Adenovirus Expressing a Soluble Fusion Protein PD-1/CD137L Subverts the Suppression of CD8$^+$ T Cells in HCC

Yonghui Zhang,[1,2,3] Hailin Zhang,[1,3] Mei Wei,[1] Tao Mou,[1] Tao Shi,[1] Yanyu Ma,[1] Xinyu Cai,[1] Yunzheng Li,[1] Jie Dong,[1] and Jiwu Wei[1]

[1]Jiangsu Key Laboratory of Molecular Medicine, Medical School of Nanjing University, 22 Hankou Road, Nanjing, Jiangsu 210093, China; [2]Henan Key Laboratory of Stem Cell Differentiation and Modification, Henan Provincial People's Hospital, 7 Weiwu Road, Zhengzhou, Henan 450003, China

Oncolytic viruses are an excellent platform for developing effective strategies in cancer immunotherapy. Several challenges remain in the use of viro-immunotherapy for cancer, such as the lack of costimulatory signals and negative regulation of immune checkpoints. In this study, we designed a novel adenovirus expressing a soluble fusion protein, programmed cell death protein 1 (PD-1)/CD137L, which contains the extracellular domains of PD-1 and CD137L at each terminus (Ad5-PC). Ad5-PC preserved the costimulatory activity of CD137L and facilitated the persistence of activated CD8$^+$ T cells. Ad5-PC induced strikingly increased antitumor activity in both ascitic and subcutaneous hepatocellular carcinoma (HCC) tumor models, with 70% and 60% long-term cure rates, respectively. The improved antitumor effect of Ad5-PC was attributed to the sustained high-level lymphocyte activation and interferon (IFN)-γ production in the tumor microenvironment, and was essentially dependent on CD8$^+$ T cells rather than natural killer (NK) cells. Moreover, Ad5-huPC-expressing human soluble PD-1/CD137L fusion protein was effective in suppressing tumor growth and improving survival in a humanized mouse model. We confirmed that Ad5-PC induced tumor-specific and systematic protection against tumor rechallenges at both *in situ* and distant sites. Thus, Ad5-PC harnesses several distinct functions to efficiently overcome several major hurdles of viro-immunotherapy.

INTRODUCTION

Cancer remains one of the major health problems worldwide. Exploiting the immune system's capacity to identify and eradicate tumors has reached an important turning point in the history of cancer therapy, and remarkable progress has been made in clinical applications. A major hurdle for this strategy is the suppressive tumor microenvironment (TME) due to its complex structures and multiple components,[1] e.g., lack of lymphocytic infiltrates, insufficient costimulatory factors, or the immune negative feedback loop (immune checkpoints).

Oncolytic viruses (OVs) are a class of self-replicating viruses that selectively replicate in malignant cells, leading to cell lysis. Accumulated evidence from the last decade shows that OVs provide an excellent platform to develop next-generation immunotherapy drugs for cancer therapy.[2] Adenovirus is a double-stranded DNA virus with approximately 52 human serum types. The E1B 55-kDa-mutated type V adenovirus has been approved by the Chinese Food and Drug Administration (CFDA) for head and neck tumor therapy. Adenovirus type V with an E1B 55-kDa deletion cannot inactivate p53 and thereby is unable to replicate efficiently in normal cells.[3,4] However, in cancer cells with a p53 mutation, the virus with a E1B 55-kDa deletion can replicate efficiently and induce oncolysis. OVs possess distinct advantages in activating immune responses, such as recruitment of lymphocytes, capacity to turn cold tumors hot, induction of immunogenic cell death, and expression of modified genes that regulate the otherwise suppressive immune microenvironment. Nevertheless, the use of OVs also has challenges, such as the induction of an immunosuppressive feedback loop, e.g., programmed cell death protein 1 (PD-1)/ programmed death ligand-1 (PD-L1), or lack of immune costimulators, e.g., CD137L. Recently, it has become increasingly popular to combine various strategies to improve the efficacy of OV therapy.[5]

PD-1, one of the checkpoint inhibitors expressed by T cells, is a central regulator of T cell exhaustion and has been recently been shown to be effective in the treatment of different cancers.[6] However, the objective clinical response rates are still too low for the majority of patients, despite the impressive outcomes with PD-1 signal blockade.[7–9] Further studies showed that the expression of PD-L1 in the TME, immune cell infiltration, interferon (IFN)-γ production, and the extent

Received 2 April 2019; accepted 31 July 2019;
https://doi.org/10.1016/j.ymthe.2019.07.019.

[3]These authors contributed equally to this work.

Correspondence: Jiwu Wei, MD, Jiangsu Key Laboratory of Molecular Medicine, Medical School of Nanjing University, 22 Hankou Road, Nanjing, Jiangsu 210093, China.
E-mail: wjw@nju.edu.cn
Correspondence: Jie Dong, PhD, Jiangsu Key Laboratory of Molecular Medicine, Medical School of Nanjing University, 22 Hankou Road, Nanjing, Jiangsu 210093, China.
E-mail: dongjie@nju.edu.cn

of tumor necrosis were correlated with objective response rates to anti-PD-1 agents.[10,11] There is still an unmet need to develop combined or alternative treatments for patients with cancer that is refractory to PD-1 blockade antibodies.

CD137, a surface glycoprotein of the tumor necrosis factor receptor (TNFR) family, can be induced on a variety of leukocyte subsets. CD137L is the only known intercellular ligand for CD137. CD137 is upregulated on activated T cells, and the subsequent ligation of CD137 with its cognate ligand provides costimulatory signals for T lymphocytes,[12] leading to enhanced proliferation, reduced apoptosis, and increased IL-2 production and effector functions.[13–15] CD137 signaling promotes cytotoxic T lymphocyte (CTL) infiltration into the malignant tissue and enhances the cytotoxic functions against the tumor.[16] These functional properties of CD137 have spurred fruitful research on its use in cancer immunotherapy. Recently, genetically engineered T cells with a CD137 signaling domain have become a prominent strategy in cancer therapy.[17] *In vivo* administration of agonistic CD137 antibodies led to regression of some tumors.[18] However, systemic immune toxicity limited its clinical application.[19]

Here, we introduce a novel replication-competent adenovirus expressing a bispecific fusion protein, which contains the extracellular domain of PD-1 on one end and the extracellular domain of CD137L on another (PD1/CD137L). Our study suggests that this genetically engineered adenovirus promotes immune cell infiltration into the tumor sites. Moreover, PD1/CD137L activates tumor-specific CTLs by signaling through the CD137 pathway and blocks the PD-L1/PD-1 pathway in CTLs to diminish T cell exhaustion. Ultimately, the recombinant adenovirus mediates a markedly enhanced antitumor immune response and durable tumor regression.

RESULTS

Replicative Adenovirus Improves the Immune Responses in TME but Fails to Prolong Survival in an HCC Ascites Mouse Model

To investigate whether the oncolytic adenovirus has a therapeutic effect on malignant tumors, we constructed a replication-competent type V adenovirus (Ad5con) with an additional early region 1A (E1A) replication element (Figure 1A). The replication and oncolytic capabilities of Ad5con were confirmed in several types of tumor cells (Figure S1). The H22-based hepatocellular carcinoma (HCC) ascites mouse model was also employed to evaluate the antitumor activity of Ad5con and its influence on the TME (Figure 1B). We further monitored the dynamic changes in ascites associated with the therapeutic outcome in each mouse. As a result, both the concentration of IFN-γ and the number of IFN-γ–producing cells in ascites were significantly increased when H22-bearing mice were treated with oncolytic adenovirus (Figures 1C and 1D). In addition, $CD8^+$ T cells and NK1.1 cells were recruited into ascites after Ad5con treatment (Figure 1E). However, survival did not improve in the Ad5con group compared with the untreated group (Figure 1G). Interestingly, PD-L1, an immunosuppressive molecule, was dramatically upregulated on the surfaces of ascitic cells in mice treated with Ad5con (Figure 1H).

These data suggest that the oncolytic Ad5con induces a moderate immune response at the tumor sites, which may transform the tumor from "cold" into "hot." Unfortunately, Ad5con treatment was insufficient to produce an effective antitumor effect, which may be substantially due to the elevated expression of PD-L1 on tumor cells.

Generation of a Novel Recombinant Adenovirus Regulating PD-L1/PD-1 Negative Feedback Signaling and CD137L/CD137 Costimulatory Signaling

To elicit a therapeutic antitumor immune response, we aimed to generate a novel recombinant adenovirus that blocks PD-L1/PD-1 negative feedback and provides a costimulatory signal to immune effector cells. To this end, a soluble fusion protein, PD-1/CD137L, was designed that contains the extracellular domain of PD-1 in the N terminus and the extracellular domain of CD137L in the C terminus (Figure 2A). The soluble fusion protein readily conjugates PD-L1 on tumor cells; hence the PD-1 signal in immune effector cells is blocked, and their antitumor activity can be sustained. Soluble CD137L (sCD137L) was employed to enhance T cell proliferation and cytolytic activity. The expression fragments were inserted into the genome of a replicative adenovirus. First, we confirmed that the soluble PD-1 (sPD-1), CD137L, or PD-1/CD137L fusion protein could be secreted into and accumulated in the supernatants of the virus-infected HCC cell lines (Figures 2B–2E). Of note, the replicating and oncolytic activities of the recombinant adenovirus were not impaired in the presence of any one of the soluble proteins (Figures 2F–2K). These data suggested that the recombinant adenovirus expressing the fusion protein retained its capabilities for replication and oncolysis while producing and secreting soluble fusion protein.

Recombinant Ad5-PD-1/CD137L (Ad5-PC) Markedly Induces Immune Responses and Increases the Durable Cure Rate

In an HCC ascites mouse model, we investigated the antitumor efficacy of recombinant AD5-PC. The tumor model and the therapeutic regimen are depicted in Figure 3A. Survival of the mice treated with control virus (Ad5con) or with virus encoding a sPD-1 (extracellular domain of PD-1, Ad5-P) was comparable with that of the mice that received saline. Furthermore, the sCD137L-producing adenovirus (Ad5-C) significantly prolonged mouse survival and led to an approximately 30% cure rate. Surprisingly, there was a 70% cure rate in mice treated with Ad5-PC, which was even better than the cure rate in mice treated with the Ad5-P and Ad5-C combination (Figure 3B). We also monitored the respective soluble protein levels and viral replication in ascites during treatment at earlier stages and found no significant differences (Figure 3C). Moreover, the IFN-γ-producing immune cells in ascites were characterized on days 14 and 19. All viruses effectively activated immune responses, and a relatively higher level was achieved by both Ad5-C

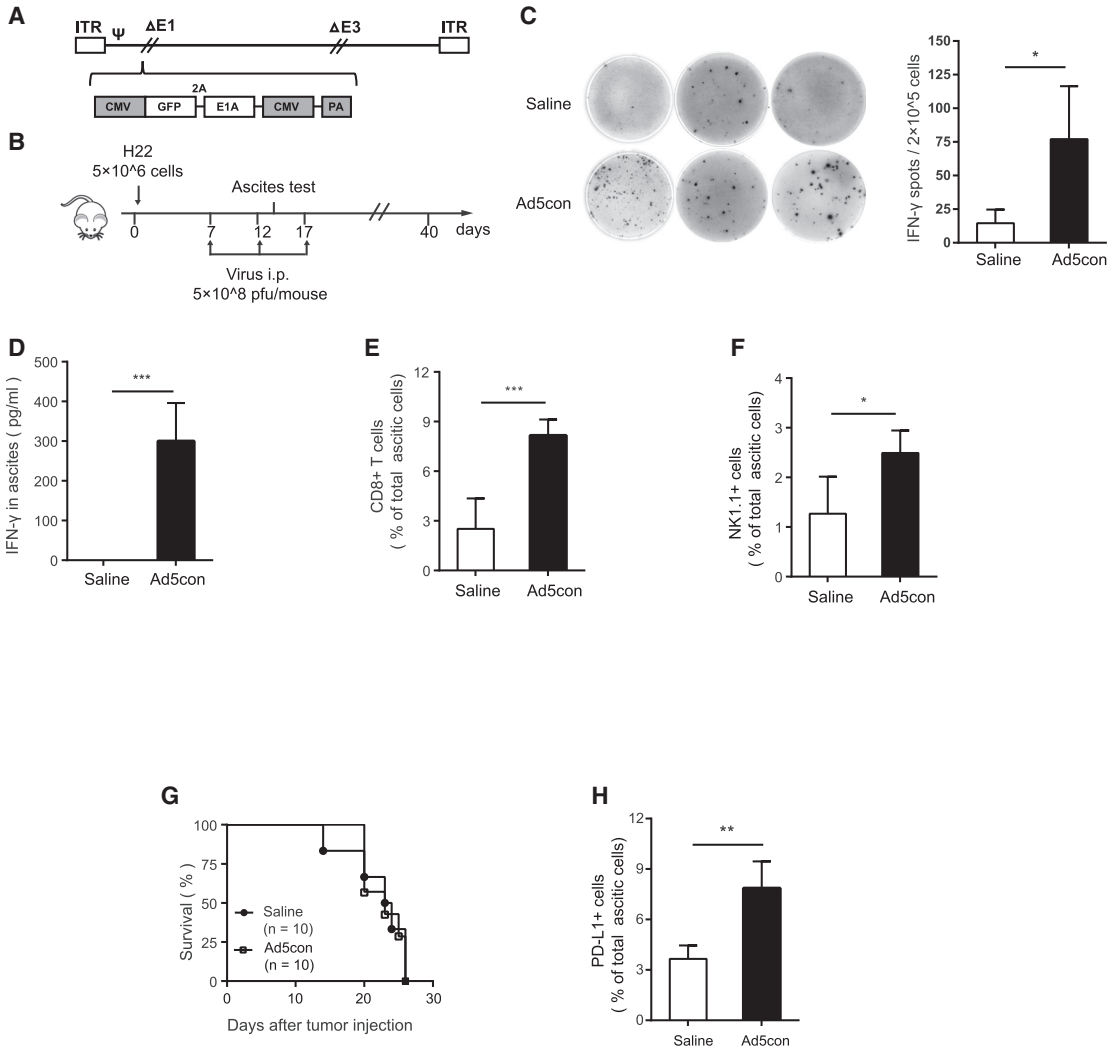

Figure 1. Replication-Competent Adenovirus Improves Immune Responses in TME but Fails to Prolong Survival in an Ascitic HCC Murine Model

Male C57BL/6 mice were injected peritoneally with 5×10^6 H22 cells. On days 7, 12, and 17, mice were treated i.p. with Ad5con (5×10^8 PFUs), with saline used as a control (n = 10 for each group). (A) Construction of the replication-competent adenovirus. (B) Schematic diagram of the experimental setup for adenovirus therapy. (C) Mouse ascites were collected on day 14, and the IFN-γ-producing lymphocytes were determined by ELISpot. The representative results for ELISpot are shown in the left panel, and the associated plot counts are shown in the right panel. (D) IFN-γ concentrations in the ascites were determined by ELISA. (E and F) Frequencies of (E) $CD8^+$ T cells and (F) NK cells were determined by flow cytometry. (G) Survival curves of mice with or without Ad5con treatment. (H) PD-L1-positive cells in ascites were detected by flow cytometry. Data shown are the means ± SD. Data are representative of at least three independent experiments. *$p < 0.05$, **$p < 0.01$, ***$p < 0.001$.

and Ad5-PC on day 14. Interestingly, on day 19, immune activation was markedly decreased in ascites treated with Ad5-C, whereas immune activation was sustained in ascites treated with Ad5-PC (Figure 3D). Consistent with these findings, increased $CD8^+$ T cell infiltration levels were found in ascites treated with both viruses, and again, the number of $CD8^+$ T cells was markedly reduced in ascites treated with Ad5-C, whereas it was sustained in ascites treated with Ad5-PC over time (Figure 3E). These data suggest that sCD137L (a costimulatory molecule) could induce an intense immune activation, and that sPD-1 is required to maintain a high-level immune activation.

Taken together, these results showed that Ad5-PC not only robustly activated immune responses but also successfully sustained immune activation at a relatively high level, which was sufficient to eradicate tumor cells.

$CD8^+$ T Cells Mediate the Antitumor Effect of Ad5-PC

Next, we depleted $CD8^+$ T or natural killer (NK) cells in HCC ascites mice using anti-NK1.1 or anti-CD8a antibodies, respectively (Figure 4A). NK1.1 and $CD8^+$ T cells were rarely found in the peripheral blood from mice after injection with anti-NK1.1 or anti-CD8 antibodies, respectively (Figure 4B). The antitumor

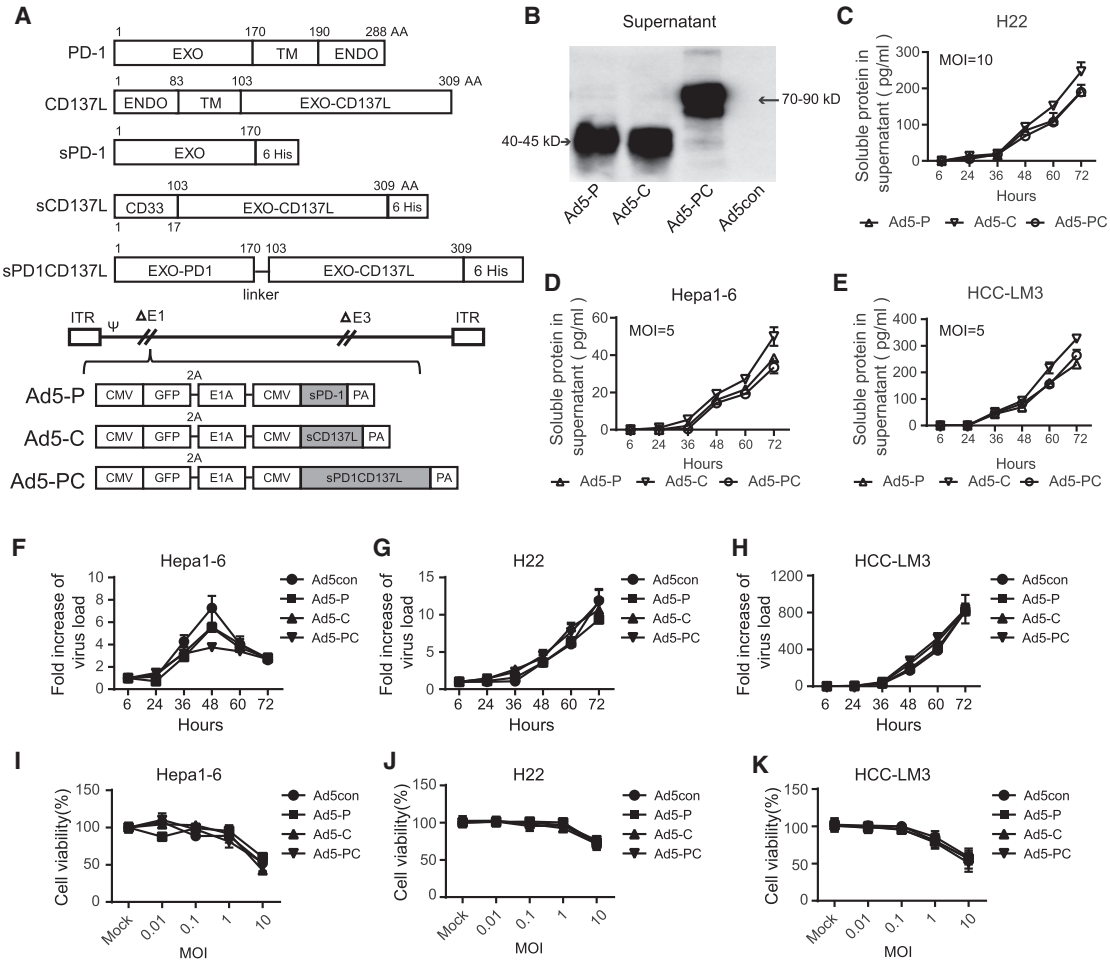

Figure 2. Generation of Recombinant Adenoviruses Regulating PD-L1/PD-1 Negative Feedback Signaling and CD137L/CD137 Costimulatory Signaling

Recombinant adenoviruses were generated to secrete soluble PD-1 (sPD-1), soluble CD137L (sCD137L), or a fusion PD-1/CD137L (sPD-1CD137L). (A) Recombinant adenovirus constructs. (B) H22 cells were infected with recombinant adenovirus (MOI = 20) for 72 h, and the levels of sPD-1, sCD137L, and sPD-1CD137L in the supernatant were detected by western blot. The molecular weights were as expected. H22 (C), Hepa1-6 (D), and HCC-LM3 cells (E) were infected with recombinant adenoviruses at MOIs of 20 or 5. The supernatants were collected at the indicated time points, and the concentrations of soluble proteins were determined by ELISA. H22 cells (F), Hepa1-6 cells (G), and HCC-LM3 cells (H) were infected with recombinant adenoviruses at an MOI of 10 and harvested at varying time points. DNA was extracted, and the viral copy number was determined by qPCR. The fold changes were calculated by dividing the copy number at 6 h. H22 cells (I), Hepa1-6 cells (J), and HCC-LM3 cells (K) were infected with recombinant adenoviruses at the indicated MOI for 72 h, and cell viability was determined by MTT. Data shown are the means ± SD. Ad5-C, recombinant adenovirus encoding sCD137L; Ad5-P, recombinant adenovirus encoding sPD-1; Ad5-PC, recombinant adenovirus encoding sPD-1CD137L; ENDO, endocellular domain; EXO, extracellular domain; TM, transmembrane region.

efficacy of Ad5-PC was completely abrogated in mice lacking $CD8^+$ T cells, whereas it was not impaired by the anti-NK1.1 antibody (Figure 4C). A comparable level of sPD-1/CD137L (Figure 4D) and a similar viral copy number (Figure 4E) were found in the murine ascites, which ruled out the possible impact of the blocking antibodies on viral expression and/or viral replication. Interestingly, the concentration of IFN-γ was significantly reduced in ascites in the presence of the anti-CD8a antibody (Figure 4F), suggesting that $CD8^+$ T cells were a critical source of IFN-γ, which was indispensable for Ad5-PC-induced antitumor immunity.

These results indicate that $CD8^+$ T cells, rather than NK1.1 cells, mediate the antitumor effect.

Ad5-PC Suppresses Tumor Growth in a Solid Tumor Model

We then studied the antitumor efficacy of Ad5-PC in a solid HCC mouse model (Figure 5A). Compared with the group treated with saline or Ad5con, intratumoral injection of Ad5-PC significantly reduced the tumor burden (Figure 5B) and markedly prolonged the lifespan (Figure 5C). In fact, 6 out of 10 mice were cured by treatment with Ad5-PC (Figures 5C–5F). We also determined the level of the soluble fusion protein PD-1/CD137L and the level of serum IFN-γ in the

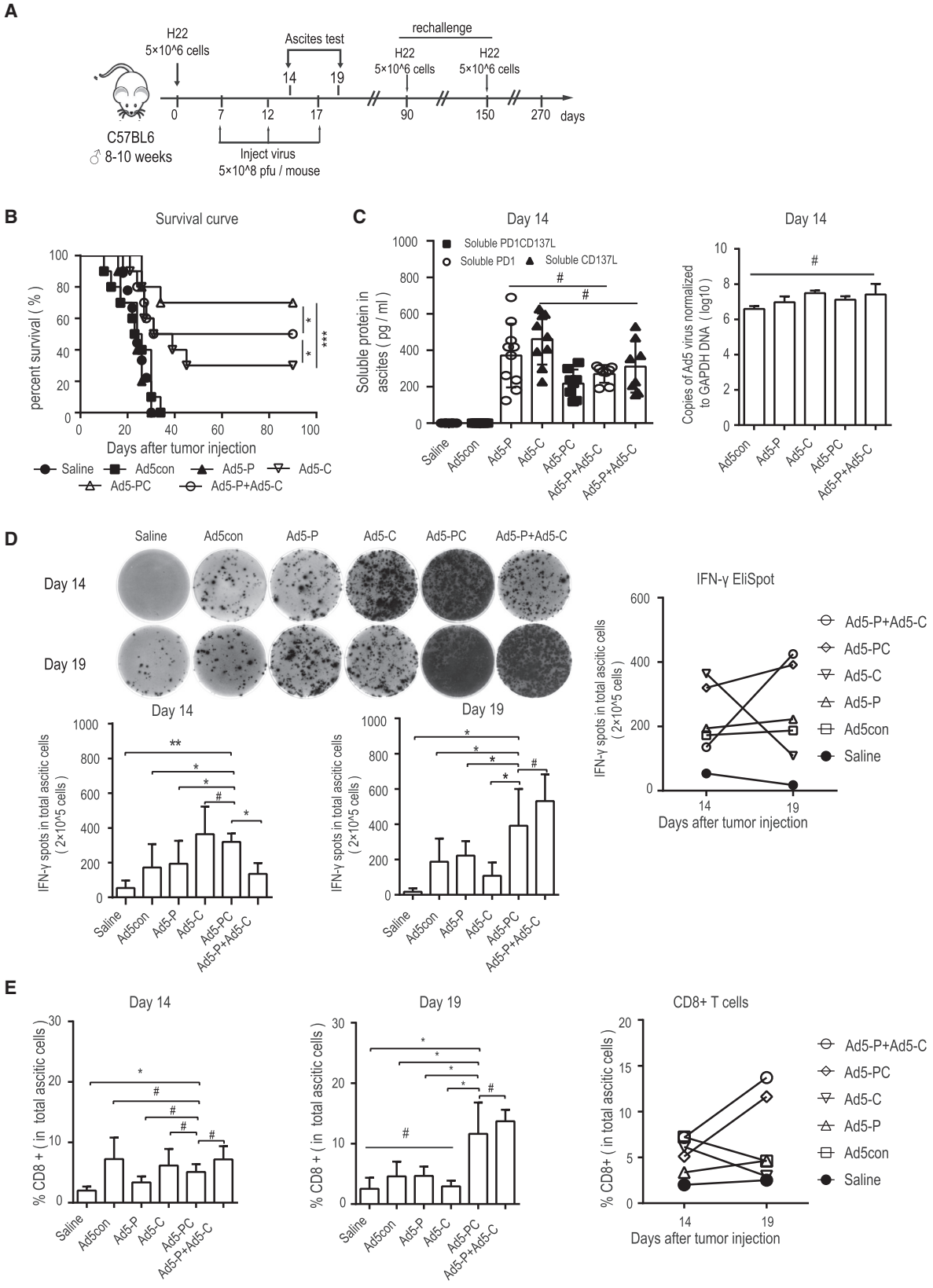

(legend on next page)

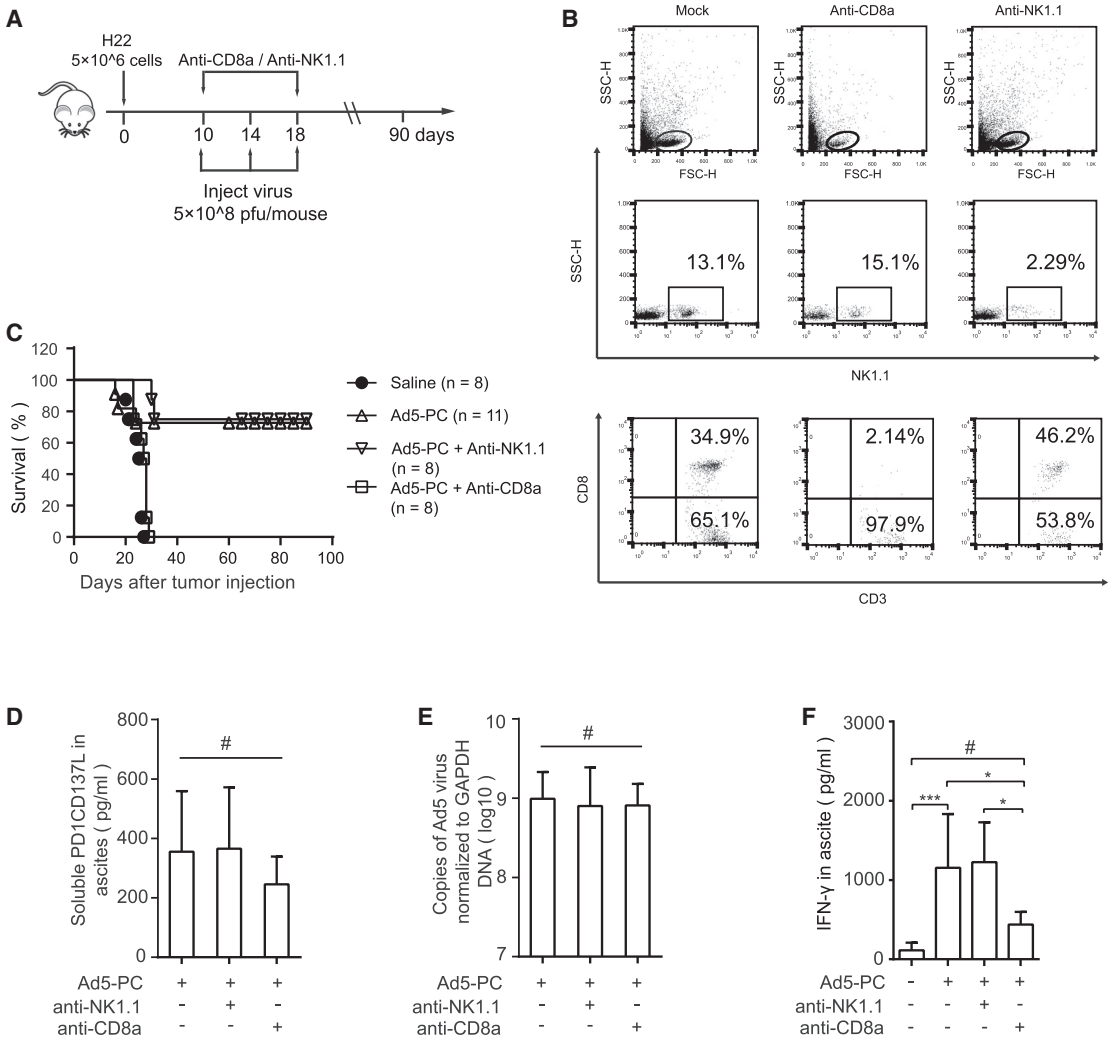

Figure 4. CD8⁺ T Cells Mediate the Antitumor Activity of Ad5-PC

Male C57BL/6 mice were injected peritoneally with 5×10^6 H22 cells. Mice were treated i.p. with recombinant adenoviruses (5×10^8 PFUs/mouse), combined with or without anti-CD8a or anti-NK1.1. (A) Schematic diagram of the experimental setup for CD8⁺ T cell or NK cell depletion. (B) Mouse blood was collected 5 days after the administration of blocking antibody, and the depletion effects of anti-CD8a and anti-NK1.1 were confirmed via flow cytometry. (C) Survival curves of mice treated with recombinant adenoviruses in the presence or absence of anti-CD8a or anti-NK1.1 antibodies. The concentrations of soluble proteins (D) and IFN-γ (F) in ascites were determined by ELISA. (E) Viral copies in ascites were detected by qPCR. Data shown are the means ± SD. #Not significant; *p < 0.05, ***p < 0.001.

peripheral blood. The fusion protein PD-1/CD137L was hardly found in blood (data not shown), and Ad5-PC did not cause a significant increase in serum IFN-γ, indicating that local administration of Ad5-PC may decrease the chance of systemic immune-related side effects (Figure 5G). In addition, OV treatment had no influence on mouse weight (Figure 5H). To evaluate the effect of fusion protein PD-1/CD137L on immune moderation, we purified the secreted proteins from the supernatant. As shown in Figure 5I, the splenic cells displayed a dramatically increased capacity for tumor killing in the presence of the PD-1/CD137L protein compared with PD1 or CD137L treatment.

Figure 3. Recombinant Ad5-PD-1/CD137L Activates Immune Responses and Increases Durable Cure Rate

Male C57BL/6 mice were injected peritoneally with 5×10^6 H22 cells. On days 7, 12, and 17, mice were treated i.p. with recombinant adenoviruses (5×10^8 PFUs), and ascites were collected on days 14 and 19 (n = 10 for each group). (A) Schematic diagram of the experimental setup for adenovirus therapy. (B) Survival curves of mice treated with recombinant adenoviruses. (C) On day 14, the concentrations of soluble proteins in ascites were detected by ELISA, and viral copies were determined by qPCR. Data shown are the means ± SD. (D) On days 14 and 19, the IFN-γ-producing lymphocytes in ascites were determined by ELISpot. The representative results are shown in the left panel, and the associated plot counts are shown in the right panel. (E) CD8⁺ T cell frequencies in ascites were determined by flow cytometry. Data shown are the means ± SD. #p value was not significant; *p < 0.05, **p < 0.01, ***p < 0.001.

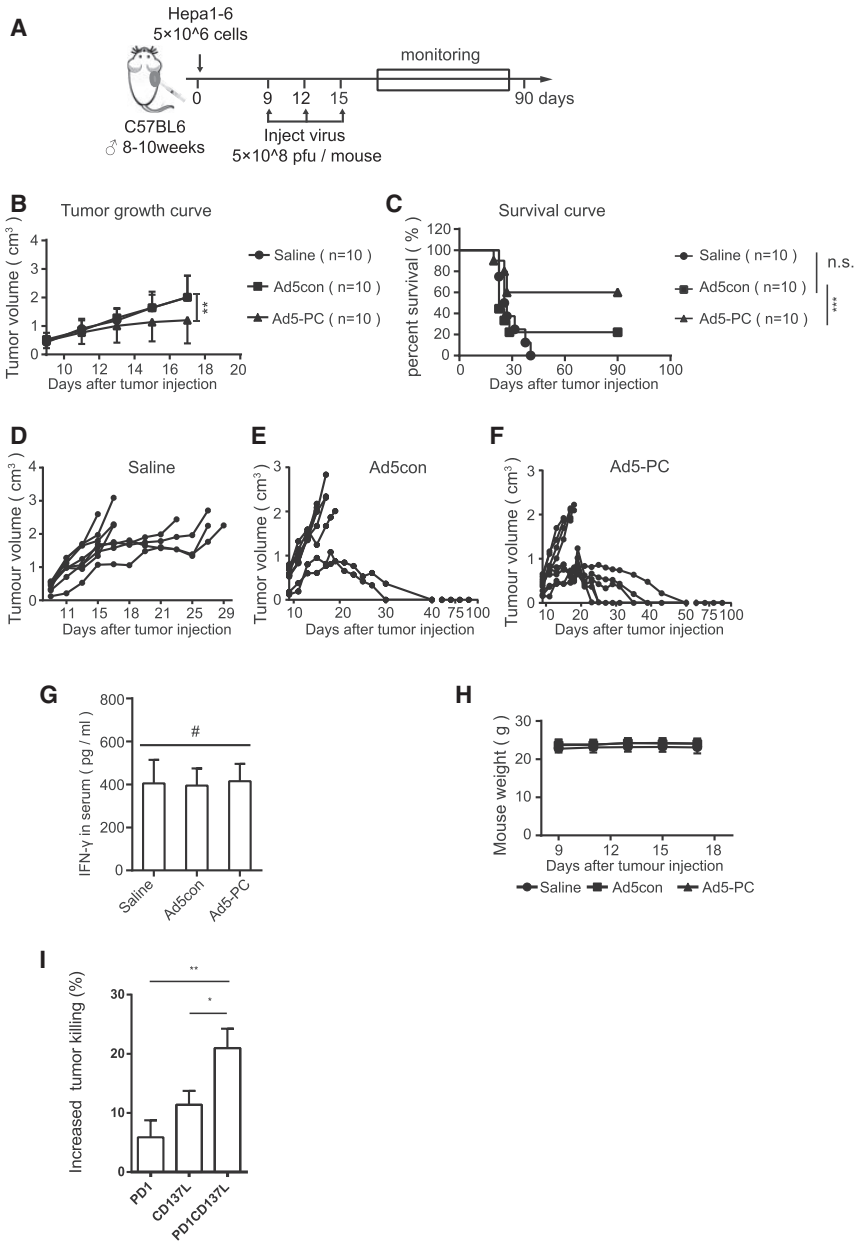

Figure 5. Ad5-PC Attenuates Tumor Growth in a Subcutaneous HCC Murine Model

Male C57BL/6 mice were subcutaneously inoculated with 5×10^6 Hepa1-6. Recombinant adenovirus (5×10^8 PFUs/mouse) was locally injected when the tumor volume reached 0.4 cm^3. The tumor volume and mouse weights were monitored, and the mice were considered to have died when the tumor volume reached 2 cm^3. (A) Schematic diagram of the experimental setup for adenovirus therapy in solid tumors. Tumor volumes (B) and survival curves (C) of mice with or without treatment of recombinant adenovirus were determined. (D–F) Volume for each tumor in the group of mice treated with (D) saline, (E) Ad5con, or (F) Ad5-PC. (G) On day 14, the concentrations of sPD-1CD137 and IFN-γ in plasma were determined by ELISA. (H) Mouse weights were determined at the indicated time points. (I) Splenocytes and Hepa1-6 were mixed at a ratio of 5:1, in the presence of purified PD1, CD137L, or fusion protein PD1/CD137L, respectively. The number of Hepa1-6 cells was reflected by the bioluminescence intensity. Data shown are the means ± SD. #Not significant; *$p < 0.05$, **$p < 0.01$, ***$p < 0.001$.

These findings show that Ad5-PC induces a sufficient antitumor effect in solid tumors with limited spread of the fusion protein in blood. The tumor killing promoted by the fusion protein may be a partial explanation for the Ad5-PC-mediated antitumor responses.

Ad5-PC Induces Tumor-Specific and Long-Term Immune Memory in Mice

To elucidate whether the Ad5-PC-mediated tumor clearance was tumor specific, the cured H22-bearing mice were rechallenged with two rounds of peritoneal injections with H22 cells, and no tumor burden (ascites) was observed, whereas all naive mice were susceptible to the challenge with H22 cells (Figure 6A). This finding indicated that Ad5-PC elicits long-term antigen-specific immune memory.

Furthermore, cured mice from both H22 and Hepa1-6 models were subcutaneously injected with H22 cells. As shown in Figure 6B, H22 cells rapidly developed into solid tumors in mice that had survived a Hepa1-6 challenge, whereas mice that had survived a H22 challenge were resistant to the subsequent rechallenge with H22 cells. These data suggest that the antitumor effect induced by Ad5-PC was tumor specific.

Ad5-huPC Has a Therapeutic Effect in a Humanized Mouse Model

Finally, we aimed to elucidate whether Ad5-PC also effectively activates the antitumor immune responses in human immune cells. To this end, adenovirus encoding a fusion protein with human PD1 and CD137L extracellular domain (Ad5-huPC) was generated (Figure 7A) and transplanted with human HCC-LM3 cells in non-obese diabetic (NOD)-SCID IL-2 receptor gamma null (NSG) mice transfused with human peripheral blood mononuclear cells (PBMCs) (Figure 7B). Consistent with previous results, tumor growth was inhibited in mice that had received Ad5-huPC (Figure 7C). Ad5-huPC administration led to significantly improved survival in LM3-bearing mice (Figure 7D). These results indicate that Ad5-huPC is sufficient to activate human immune cells and induce antitumor responses.

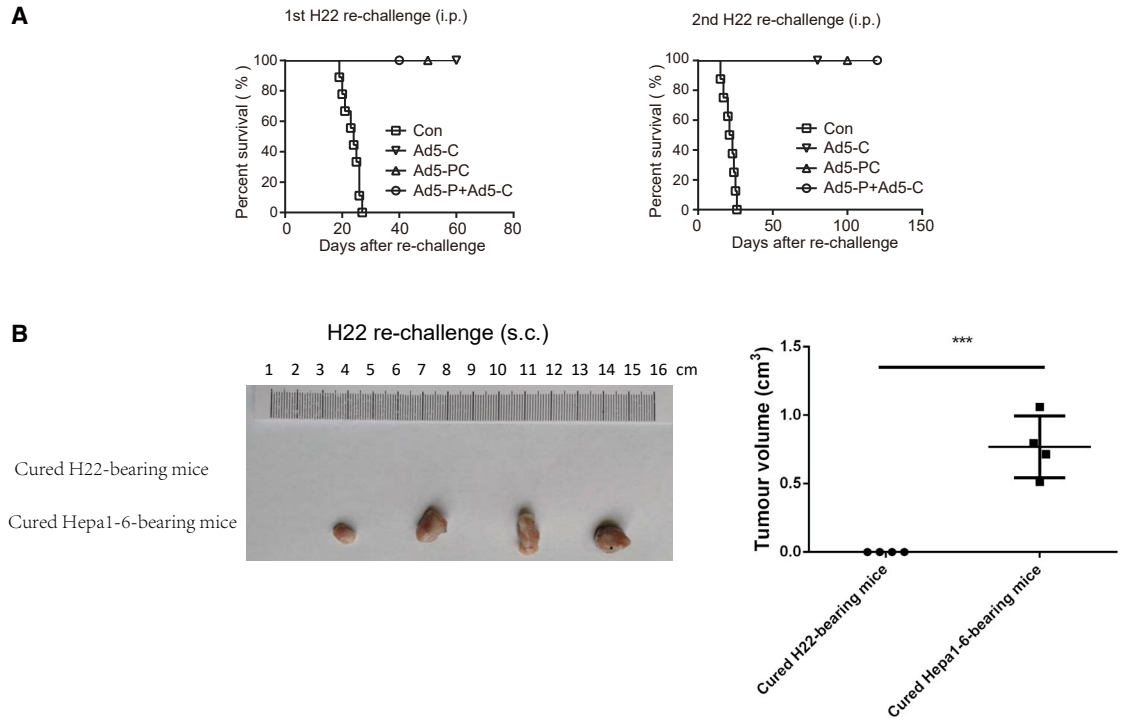

Figure 6. Ad5-PC-Cured Mice Exhibit a Tumor-Specific and Long-Term Immune Memory

(A) Mice that had been cured were re-challenged with 5×10^6 H22 cells on days 90 and 150 post-inoculation. Naive mice were used as a control. The day that mice received the re-challenge was regarded as day 0 in the survival curves. (B) Cured mice from H22 ascetic tumor or hepa1-6 solid HCC were subcutaneously injected with 5×10^6 H22 cells. Mice were sacrificed for tumor measure 16 days after re-challenge with H22 cells. i.p., injected peritoneally; s.c., injected subcutaneously. ***$p < 0.001$.

A Model Depicting How Ad5-PC Overcomes the Hurdles of Immune Activation

The presence of coinhibitory checkpoints and the absence of costimulatory signals compromise virus-induced immune activation (Figure 8, left). Adenovirus infection induces lymphocyte infiltration in TME, after which the soluble fusion protein PD-1/CD137L provides an indispensable activation signal to CTLs by the CD137L/CD137 interaction and further sustains the immune activity of CTLs by blocking the PD-1/PD-L1 interaction. In addition, sPD-1/CD137L may bridge the gap between effector T cells and malignant cells to enhance cytotoxicity (Figure 8, right).

DISCUSSION

Oncolytic viro-immunotherapy has made remarkable progress in clinical cancer therapy.[20] In this study, we generated a novel replication-competent adenovirus that produces a bispecific fusion protein containing the extracellular domain of PD-1 and the extracellular domain of CD137L (Ad5-PC). The oncolytic Ad5-PC harnesses multiple antitumor activities to overcome several major hurdles in viro-immunotherapy. In ascitic and solid HHC tumor models, Ad5-PC administration achieved 70% and 60% cure rates, respectively. Furthermore, $CD8^+$ T cells mediated the antitumor activity induced by Ad5-PC.

Although the replication-competent adenovirus alone induced immune responses in tumor sites, it was not sufficient to improve the outcomes in a murine HCC ascites model. We hypothesized that the virally mediated upregulation of PD-L1 expression might have contributed to immune inhibition because some reports have shown that OV infection upregulated PD-L1.[21–23] Indeed, some studies have shown that OVs combined with systemic immune checkpoint blockade improved antitumor efficacy.[24–26] The oncolytic measles virus (MV) armed with a PD-L1 antagonist showed an equal antitumor efficacy as MV in combination with systemic administration of PD-L1 in melanoma treatment.[27] Surprisingly, Ad5-P did not improve the antitumor effect in HCC ascites compared with control adenoviruses. It is likely that blocking the immune negative feedback alone, such as with PD-1/PD-L1 in the TME, is not sufficient to elicit effective antitumor responses. Another explanation is the lack of costimulatory signals for CTL activation.

CD137L is a costimulatory molecule and provides the second activation signal for T lymphocytes through binding to its receptor, CD137.[12] $CD137^+$ tumor infiltrated lymphocytes (TILs) displayed a stronger response to tumor antigens. The cytoplasmic tail of CD137 has been integrated into CAR T cells to transmit activation signals.[28,29] In fact, OVs armed with a costimulatory molecule, e.g., CD137L and OX40L, shaped the immune response in the TME and facilitated the induction of tumor-specific and long-lasting antitumor responses.[30,31] In the current study, adenovirus expressing the costimulatory molecule CD137L (Ad5-C) strongly activated immune

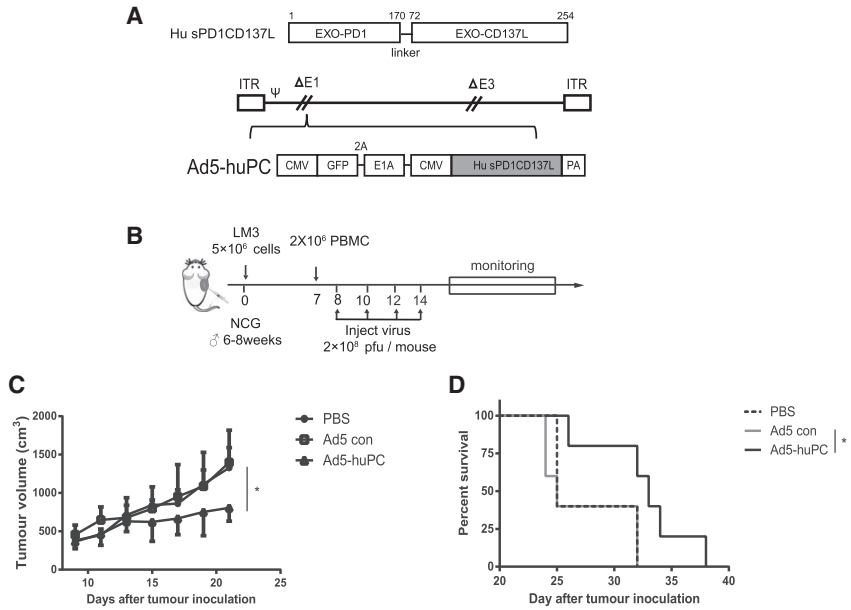

Figure 7. Ad5-huPC Significantly Inhibits HCC Growth and Prolongs Survival in a Humanized Mouse Model

(A) The recombinant adenovirus coding for human PD1/CD137L. (B) Schematic diagram of the experimental setup for Ad5-PC therapy in the NCG mouse model. Male NCG mice were injected subcutaneously with 5×10^6 LM3 cells. Human PBMC was administrated on day 7, followed by the Ad5-huPC treatment. Tumor volumes (C) and mice survival (D) were monitored. *$p < 0.05$.

responses in HCC ascites compared with Ad5-P and resulted in a profound antitumor response in the HCC ascites. Our data suggest that the lack of costimulatory signals plays a pivotal role in tumor immunosuppression.

We observed that the immune activity upregulated by Ad5-C was rapidly weakened over time, indicating that the presence of costimulatory signals alone is not sufficient to elicit long-term effective immune activation. Ad5-PC induced a similar activation of the antitumor immune response as Ad5-C, suggesting that the fusion protein does not interfere with the stimulatory activity of CD137L. Importantly, Ad5-PC successfully sustained IFN-γ production and continuously increased the number of $CD8^+$ T cells in the TME, achieving the highest cure rate in the present study. Similarly, intratumoral injection of Ad5-PC achieved excellent therapeutic efficacy in a solid HCC tumor model. These data indicate that the PD-1/CD137L fusion protein is potent in activating the otherwise silent immunity and is efficient in boosting the activation of infiltrated immune cells by CD137L signaling, while prolonging the persistence of CD137L-boosted $CD8^+$ T cells by PD-1 signaling in the TME. Consistent with these results, sustained immune activity was also achieved by the combination of Ad5-P and Ad5-C in the TME, which led to an approximately 50% cure rate. Thus, to achieve an effective antitumor immune response, signals for both immune boosting and preventing immune exhaustion are indispensable.

Interestingly, Ad5-PC exhibited superior antitumor efficacy over the combination of Ad5-P and Ad5-C. The fusion protein caused a significantly increased efficacy of tumor killing in splenic cells, even stronger than that induced by PD1 and CD137L together. It has been suggested that both the perforin and Fas/FasL pathways, two primary antitumor mechanisms of CTLs, require a direct interaction between the CTL and the target cell.[32] Therefore, like other bispecific T cell engagers,[33] the PD-1/CD137L fusion protein may function as a bidirectional conjugator, which connects the CTLs and the tumor cells, leading to improved oncolysis. Moreover, PD-1/CD137L as a connection between PD-L1 and CD137 may convert the PD-1 suppressing signal to an activating signal in CTLs. Further investigations are still required to address this issue. The antitumor effect of Ad5-PC was mediated by $CD8^+$ T cells, whereas NK cells did not contribute to the antitumor immunity. Because NK cells are also important in antitumor immunity, it will be interesting to develop a combination strategy involving Ad5-PC and reagents for NK cell activation.

Until now, most OVs have been administered locoregionally either alone or in combination. Several studies showed that regional tumor administration of OVs inhibited distant tumors.[34,35] Combination therapy with intratumoral OVs and systemic checkpoint blockade promoted distant tumor infiltration of activated T cells and led to an increase in therapeutic efficacy.[26,27,36] In the current study, our goal was to identify the antitumor efficacy of the novel recombinant Ad5-PC. As a proof of principle, we performed the experiments in an ascitic and a subcutaneous HCC mouse model. Whether this strategy is relevant to the therapy of patients with metastatic disease is worthy of further thorough investigation in an appropriate animal model.

Ad5-PC displayed a distinctive capacity for tumor control in both the HCC ascites and the solid tumor models, with no side effects observed, suggesting that this method could be a promising and safe strategy for cancer immunotherapy. Given that the systemic administration of checkpoint blockade effectors frequently induces immune-related adverse events (IRAEs), the local administration of Ad5-PC, which produces a high level of sPD-1/CD137L *in situ* and limited or negligible levels of fusion protein in plasma, can reduce the chance of developing IRAEs during the course of treatment. Furthermore, the recombinant adenovirus Ad5-huPC expressing the human sPD-1/CD137L fusion protein was effective in suppressing tumor growth and prolonging the lifespan, providing more information to warrant further clinical applications.[8,37]

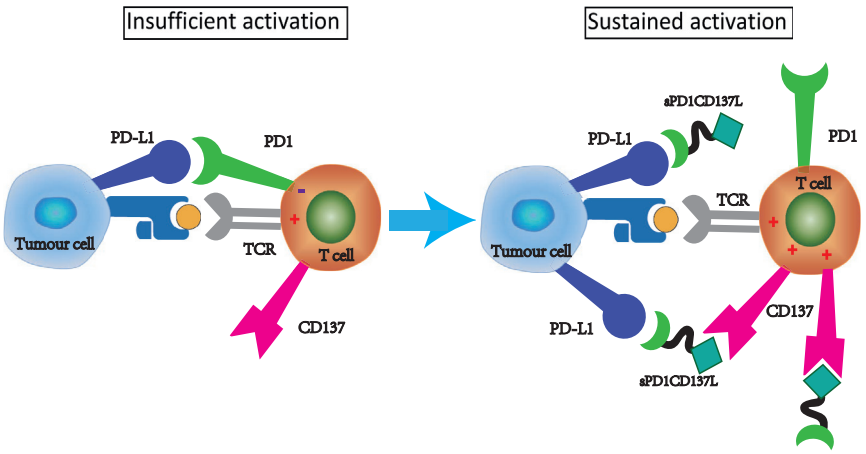

Figure 8. Ad5-PC Harnesses Multiple Distinct Functions to Improve Antitumor Immune Responses

Recombinant adenovirus producing the soluble fusion protein PD1/CD137L harnesses multiple distinct functions to promote antitumor immune responses. The infiltrated T cells induced by adenovirus are suppressed because of the inhibitory molecule PD-L1 and the paucity of costimulatory molecules (left panel). The soluble fusion protein PD1/CD137L provides a costimulatory signal to the virus-recruited $CD8^+$ T cells and sustains the immune activity of $CD8^+$ T cells by blocking PD-L1. Furthermore, sPD1/CD137L may bridge the gap of effecter T cells and malignant cells to enhance cytotoxicity and convert PD-L1-mediated suppressive signal to activating signal (right panel).

Long-term specific antitumor immune surveillance is critical for preventing tumor reoccurrence. H22-bearing mice cured by Ad5-PC were resistant to rechallenges with H22 cells both *in situ* and at distant sites, indicating that Ad5-PC induced durable and systematic immune surveillance. Interestingly, the Hepa1-6-bearing mice cured by Ad5-PC were sensitive to H22 rechallenge, indicating that the immune protection induced by Ad5-PC was tumor specific.

In summary, the Ad5-PC harnesses multiple functions to efficiently overcome the therapeutic flaws of each, i.e., insufficient immune boosting and rapid exhaustion of CTLs, and would be a promising agent for tumor immunotherapy.

MATERIALS AND METHODS

Cell Culture

The human HCC cell line HCC-LM3 and the mouse HCC cell line H22 were obtained from the China Center for Type Culture Collection, authenticated by short tandem repeat (STR) analysis, and tested for mycoplasma contamination. The mouse HCC cell line Hepa1-6, human embryonic kidney cells 293T, human alveolar adenocarcinoma cell line A549, mouse melanoma cell line B16-F10, and Lewis lung carcinoma cell line LLC1 were obtained from the American Type Culture Collection (Manassas, VA, USA). H22 cells were cultured in RPMI 1640 medium (Life Technologies), and the other cell lines were cultured in DMEM supplemented with 10% fetal bovine serum, 2 mM L-glutamine, 100 U/mL penicillin, and 0.1 mg/mL streptomycin (Thermo Fisher Scientific, GIBCO, Grand Island, NY, USA). All cells were maintained in a humidified incubator with an atmosphere containing 5% CO_2 at 37°C.

Recombinant Adenovirus Construction

Recombinant adenovirus was generated as previously described.[38] E1A cDNA was obtained from 293T cells. The cDNA encoding the extracellular domains of PD-1 and CD137L were purchased from Sino Biological. The gene fragments used in our study were generated by PCR amplification using specific primer pairs (Table S1) and were connected by ligation PCR. For the secretion of sCD137L, the CD33 signal peptide (MPLLLLLPLLWAGALAM) was designed upstream of the CD137L sequence. The prepared sequences were cloned into adenovirus shuttle plasmid pENTR Vector using the *Age*I and *Xho*I restriction sites. The recombinant adenoviral vectors expressing soluble proteins were obtained via homologous recombination between the shuttle plasmid and the adenovirus backbone pAd/PL-DEST (Thermo Fisher Scientific, Invitrogen, Carlsbad, CA, USA). After digestion with the restriction enzyme *Pac*I, the recombinant adenovirus was generated by transfecting 293T cells. The virus was then amplified in 293T cells and purified using double cesium chloride gradient ultracentrifugation. Virus titration was determined by adding serially diluted virus into a 96-well plate seeded with 293T cells (10,000 cells/well). Cells were cultured for 4 days, and fluorescence was evaluated via microscopy. The virus titer was calculated according to the following formula:

$$\mathrm{TCID}_{50} = 10^{2+(S/N-0.5)}/\mathrm{mL},$$

$$\mathrm{PFU/mL} = 0.7 \times \mathrm{TCID}_{50}/\mathrm{mL},$$

where S is the total number of fluorescence-positive wells, and N is the number of replicates.

Viral Oncolysis

Cells were seeded on a 96-well plate, and adenovirus was added at the indicated MOI. Seventy-two hours later, the cells were supplemented with 100 μL 3-(4,5-dimethyl-2-thiazolyl)-2,5-diphenyl-2-H-tetrazolium bromide, thiazolyl blue tetrazolium bromide (MTT) reagent and incubated for another 4 h. The supernatant was discarded, and 150 μL of isopropanol was added. The absorbance for each well was tested by filtering at a wavelength of 570 nm.

Viral Replication

Cells were plated on a 24-well plate and infected with adenovirus at an MOI of 2. Cells were harvested at 6, 24, 36, 48, 60, and 72 h. Then the DNA was isolated, and the viral copy number was quantified using the ViiA 7 Real-Time PCR System (Applied Biosystems, Foster,

CA, USA). The shuttle plasmid containing E1A was used to prepare the standard curve, and the primer pairs Q-E1A F and Q-EIA R (Table S1) were used for the qPCR. The fold changes were calculated from the titers at 6 h.

Mouse Tumor Models

For the HCC ascites murine model, specific pathogen-free (SPF) grade 8-week-old C57BL/6 male mice were purchased from Nanjing University Model Animal Institute. A total of 5×10^6 H22 cells were injected peritoneally to develop an ascites tumor model. On days 7, 12, and 17, mice were injected peritoneally (i.p.) with recombinant adenovirus (5×10^8 plaque-forming units [PFUs]/mouse), and saline was used as a control. The ascites were collected on days 14 and 19, and subsequent analyses were performed immediately. The mice that had been cured were rechallenged with 5×10^6 H22 cells on days 90 and 150, and naive mice were used as a negative control. To deplete the $CD8^+$ T cells and NK cells, mice were injected peritoneally with 500 μg of anti-CD8a (Bioxcell, West Lebanon, NH, USA) or anti-NK1.1 (Bioxcell, West Lebanon, NH, USA) on day 10 and received a second injection 1 week later. For survival monitoring, the mice were left untreated after the adenovirus administration, and the survival time for each mouse was recorded.

For the solid tumor model, C57BL/6 mice were subcutaneously inoculated with 5×10^6 Hepa1-6 cells. On days 9, 12, and 15, Ad5-PC or Ad5con (5×10^8 PFUs/mouse) was intratumorally injected, and saline was used as a control. Tumor volume and body weight were measured every other day. On day 14, mice were anaesthetized with Nembutal, and blood was collected from the retrobulbar vein for subsequent analysis. Mouse survival was continuously monitored. Mice were sacrificed when the tumor volume reached 2.0 cm^3. Tumor volume was calculated by V = (length × width2)/2.

For the humanized mouse model, NOD-$Prkdc^{scid}$ $Il2rg^{null}$ (NCG) mice (Nanjing University Model Animal Institute) were subcutaneously inoculated with 5×10^6 human HCC cell line LM3 cells. On day 7, human PBMCs were collected from healthy donors, isolated with Ficoll, and then intravenously injected into LM3-bearing mice (2×10^6 PBMCs/mouse). On days 8, 10, 12, and 15, Ad5-huPC or Ad5con (2×10^8 PFUs/mouse) was administered by intratumoral injection. Tumor volume and mouse survival were monitored.

All animal care and handling procedures were performed in accordance with the NIH Guide for the Care and Use of Laboratory Animals and were approved by the Institutional Review Board of Nanjing University (Nanjing, China). We strictly obeyed the Declaration of Helsinki for Medical Research involving Human Subjects during the project and obtained written consent from all subjects. This study was approved by the Ethics Committee of The Affiliated Drum Tower Hospital, Medical School of Nanjing University.

Tumoricidal Activity Measurement

293T cells were infected with Ad5-PC, Ad5-P, or Ad5-C. Soluble proteins sPD1/CD137L, sPD1, or sCD137L were purified from supernatants by nickel-affinity chromatography. The purity of proteins was confirmed by SDS-PAGE and Coomassie blue staining. Splenocytes were isolated from C57BL/6 mice and cocultured with Hepa1-6 cells containing a luciferase coding gene at a ratio of 5:1 (effector:target [E:T]). Subsequently, 200 ng/mL of purified proteins was added into the coculture system. Twenty-four hours later, the cells were lysed, and substrate (Promega, WI, USA) was added for bioluminescence determination. The number of living Hepa1-6 cells was reflected by the bioluminescence intensity. Tumor-killing efficacy was calculated by comparing the bioluminescence intensity between the protein-treated and untreated control groups.

Western Blot Analysis

Supernatants from infected cells were collected and mixed with loading buffer in the presence of 2-mercaptoethanol (2-ME) and heated at 95°C for 5 min before separation on a 10% SDS-PAGE gel. The proteins were transferred to a polyvinylidene fluoride (PVDF) membrane (Merck Millipore, MA, USA) and incubated with mouse anti-His antibody (GenScript Biotech, Nanjing, China). After washing, the membrane was probed with horseradish peroxidase (HRP)-conjugated rabbit anti-mouse IgG (GenScript Biotech, Nanjing, China) and visualized with western blot chemiluminescence reagent (Millipore, Billerica, MA, USA) using an imaging system (Sage Creation Science, Beijing, China).

ELISA

For the quantification of soluble proteins, a polystyrene microplate was precoated with His tag antibody (GenScript Biotech, Nanjing, China). One hundred microliters of supernatant or ascites was added and incubated for 2 h at 37°C. After washing, anti-PD-1 or anti-CD137L antibodies (Sino Biological, Beijing, China) and HRP-conjugated streptavidin were added, and the plate was incubated for another 2 h at 37°C. TMB was used as a substrate, and the absorbance was read at 450 nm.

The concentration of IFN-γ in the ascites or plasma was quantified using a mouse IFN-γ ELISA kit according to the manufacturer's instructions (BD Biosciences, Franklin Lakes, NJ, USA).

Flow Cytometry Analysis

Ascites and blood were collected at predefined time points, and cells were obtained by centrifugation. After washing or red blood cell lysis, the harvested cells were stained with antibodies to CD3 allophycocyanin (APC), CD8a PerCP-Cy5.5, CD4 fluorescein isothiocyanate (FITC), and CD274 phycoerythrin (PE; BD Biosciences, Franklin Lakes, NJ, USA). NK1.1 FITC was purchased from BD Biosciences or Bioss (Woburn, MA, USA). The fluorescence intensity of cells was then detected using a FACSCalibur flow cytometer (BD Biosciences, San Jose, CA, USA).

IFN-γ Enzyme-Linked Immunosorbent Spot (ELISpot) Assay

Peritoneal cells were harvested from the murine ascites at the indicated time points. The IFN-γ-expressing cells were quantified using the Mouse IFN-γ ELISpot PLUS kit (3321-2AW-Plus; Mabtech,

Nacka Strand, Sweden) according to the manufacturer's instructions. In brief, 2×10^5 cells/well were incubated in a 96-well plate at 37°C for 20 h in the presence of precoated anti-IFN-γ antibody. Cells were washed away, and biotinylated secondary antibody was added. The captured IFN-γ was visualized by adding HRP-conjugated streptavidin and TMB substrate. An ELISpot reader (Autoimmun Diagnostika, Strasberg, Germany) was used to count the positive spots in each well.

SUPPLEMENTAL INFORMATION

Supplemental Information can be found online at https://doi.org/10.1016/j.ymthe.2019.07.019.

AUTHOR CONTRIBUTIONS

J.W. and J.D. conceived the study, designed the experiments, and supervised the project. Y.Z., H.Z., M.W., T.M., T.S., Y.M., X.C., and Y.L. performed the experiments and analyzed the data. J.W., J.D., and Y.Z. wrote the manuscript. All authors critically reviewed and approved the manuscript.

CONFLICTS OF INTEREST

The authors declare no competing interests.

ACKNOWLEDGMENTS

This work was supported by the National Natural Science Foundation of China (grants 81773255, 81472820, and 81700037), Six talent peaks project in Jiangsu Province (J.W.), and the Natural Science Foundation of Jiangsu Province of China (grant BK20171098).

REFERENCES

1. O'Donnell, J.S., Teng, M.W.L., and Smyth, M.J. (2019). Cancer immunoediting and resistance to T cell-based immunotherapy. Nat. Rev. Clin. Oncol. *16*, 151–167.
2. Dyer, A., Baugh, R., Chia, S.L., Frost, S., Iris, S., Jacobus, E.J., Khalique, H., Pokrovska, T.D., Scott, E.M., Taverner, W.K., et al. (2019). Turning cold tumours hot: oncolytic virotherapy gets up close and personal with other therapeutics at the 11th Oncolytic Virus Conference. Cancer Gene Ther. *26*, 59–73.
3. Bischoff, J.R., Kirn, D.H., Williams, A., Heise, C., Horn, S., Muna, M., Ng, L., Nye, J.A., Sampson-Johannes, A., Fattaey, A., and McCormick, F. (1996). An adenovirus mutant that replicates selectively in p53-deficient human tumor cells. Science *274*, 373–376.
4. Nemunaitis, J., Ganly, I., Khuri, F., Arseneau, J., Kuhn, J., McCarty, T., Landers, S., Maples, P., Romel, L., Randlev, B., et al. (2000). Selective replication and oncolysis in p53 mutant tumors with ONYX-015, an E1B-55kD gene-deleted adenovirus, in patients with advanced head and neck cancer: a phase II trial. Cancer Res. *60*, 6359–6366.
5. Ribas, A., Dummer, R., Puzanov, I., VanderWalde, A., Andtbacka, R.H.I., Michielin, O., Olszanski, A.J., Malvehy, J., Cebon, J., Fernandez, E., et al. (2018). Oncolytic Virotherapy Promotes Intratumoral T Cell Infiltration and Improves Anti-PD-1 Immunotherapy. Cell *174*, 1031–1032.
6. Ribas, A., and Wolchok, J.D. (2018). Cancer immunotherapy using checkpoint blockade. Science *359*, 1350–1355.
7. Wolchok, J.D., Chiarion-Sileni, V., Gonzalez, R., Rutkowski, P., Grob, J.J., Cowey, C.L., Lao, C.D., Wagstaff, J., Schadendorf, D., Ferrucci, P.F., et al. (2017). Overall Survival with Combined Nivolumab and Ipilimumab in Advanced Melanoma. N. Engl. J. Med. *377*, 1345–1356.
8. Ansell, S.M., Lesokhin, A.M., Borrello, I., Halwani, A., Scott, E.C., Gutierrez, M., Schuster, S.J., Millenson, M.M., Cattry, D., Freeman, G.J., et al. (2015). PD-1 blockade with nivolumab in relapsed or refractory Hodgkin's lymphoma. N. Engl. J. Med. *372*, 311–319.
9. Hamid, O., Robert, C., Daud, A., Hodi, F.S., Hwu, W.J., Kefford, R., Wolchok, J.D., Hersey, P., Joseph, R.W., Weber, J.S., et al. (2013). Safety and tumor responses with lambrolizumab (anti-PD-1) in melanoma. N. Engl. J. Med. *369*, 134–144.
10. Powles, T., Eder, J.P., Fine, G.D., Braiteh, F.S., Loriot, Y., Cruz, C., Bellmunt, J., Burris, H.A., Petrylak, D.P., Teng, S.L., et al. (2014). MPDL3280A (anti-PD-L1) treatment leads to clinical activity in metastatic bladder cancer. Nature *515*, 558–562.
11. Herbst, R.S., Soria, J.C., Kowanetz, M., Fine, G.D., Hamid, O., Gordon, M.S., Sosman, J.A., McDermott, D.F., Powderly, J.D., Gettinger, S.N., et al. (2014). Predictive correlates of response to the anti-PD-L1 antibody MPDL3280A in cancer patients. Nature *515*, 563–567.
12. Sanchez-Paulete, A.R., Labiano, S., Rodriguez-Ruiz, M.E., Azpilikueta, A., Etxeberria, I., Bolaños, E., Lang, V., Rodriguez, M., Aznar, M.A., Jure-Kunkel, M., and Melero, I. (2016). Deciphering CD137 (4-1BB) signaling in T-cell costimulation for translation into successful cancer immunotherapy. Eur. J. Immunol. *46*, 513–522.
13. DeBenedette, M.A., Chu, N.R., Pollok, K.E., Hurtado, J., Wade, W.F., Kwon, B.S., and Watts, T.H. (1995). Role of 4-1BB ligand in costimulation of T lymphocyte growth and its upregulation on M12 B lymphomas by cAMP. J. Exp. Med. *181*, 985–992.
14. Zhou, Z., Kim, S., Hurtado, J., Lee, Z.H., Kim, K.K., Pollok, K.E., and Kwon, B.S. (1995). Characterization of human homologue of 4-1BB and its ligand. Immunol. Lett. *45*, 67–73.
15. Lee, H.W., Park, S.J., Choi, B.K., Kim, H.H., Nam, K.O., and Kwon, B.S. (2002). 4-1BB promotes the survival of CD8+ T lymphocytes by increasing expression of Bcl-xL and Bfl-1. J. Immunol. *169*, 4882–4888.
16. Weigelin, B., Bolaños, E., Teijeira, A., Martinez-Forero, I., Labiano, S., Azpilikueta, A., Morales-Kastresana, A., Quetglas, J.I., Wagena, E., Sánchez-Paulete, A.R., et al. (2015). Focusing and sustaining the antitumor CTL effector killer response by agonist anti-CD137 mAb. Proc. Natl. Acad. Sci. USA *112*, 7551–7556.
17. Rosenberg, S.A., and Restifo, N.P. (2015). Adoptive cell transfer as personalized immunotherapy for human cancer. Science *348*, 62–68.
18. Cabo, M., Offringa, R., Zitvogel, L., Kroemer, G., Muntasell, A., and Galluzzi, L. (2017). Trial Watch: Immunostimulatory monoclonal antibodies for oncological indications. OncoImmunology *6*, e1371896.
19. Segal, N.H., Logan, T.F., Hodi, F.S., McDermott, D., Melero, I., Hamid, O., Schmidt, H., Robert, C., Chiarion-Sileni, V., Ascierto, P.A., et al. (2017). Results from an Integrated Safety Analysis of Urelumab, an Agonist Anti-CD137 Monoclonal Antibody. Clin. Cancer Res. *23*, 1929–1936.
20. Pol, J., Kroemer, G., and Galluzzi, L. (2015). First oncolytic virus approved for melanoma immunotherapy. OncoImmunology *5*, e1115641.
21. Liu, Z., Ravindranathan, R., Kalinski, P., Guo, Z.S., and Bartlett, D.L. (2017). Rational combination of oncolytic vaccinia virus and PD-L1 blockade works synergistically to enhance therapeutic efficacy. Nat. Commun. *8*, 14754.
22. Guo, Z.S., Liu, Z., Kowalsky, S., Feist, M., Kalinski, P., Lu, B., Storkus, W.J., and Bartlett, D.L. (2017). Oncolytic Immunotherapy: Conceptual Evolution, Current Strategies, and Future Perspectives. Front. Immunol. *8*, 555.
23. Yan, X., Wang, L., Zhang, R., Pu, X., Wu, S., Yu, L., Meraz, I.M., Zhang, X., Wang, J.F., Gibbons, D.L., et al. (2017). Overcoming resistance to anti-PD immunotherapy in a syngeneic mouse lung cancer model using locoregional virotherapy. OncoImmunology *7*, e1376156.
24. Shindo, Y., Yoshimura, K., Kuramasu, A., Watanabe, Y., Ito, H., Kondo, T., Oga, A., Ito, H., Yoshino, S., Hazama, S., et al. (2015). Combination immunotherapy with 4-1BB activation and PD-1 blockade enhances antitumor efficacy in a mouse model of subcutaneous tumor. Anticancer Res. *35*, 129–136.
25. Ilett, E., Kottke, T., Thompson, J., Rajani, K., Zaidi, S., Evgin, L., Coffey, M., Ralph, C., Diaz, R., Pandha, H., et al. (2017). Prime-boost using separate oncolytic viruses in combination with checkpoint blockade improves anti-tumour therapy. Gene Ther. *24*, 21–30.
26. Zamarin, D., Ricca, J.M., Sadekova, S., Oseledchyk, A., Yu, Y., Blumenschein, W.M., Wong, J., Gigoux, M., Merghoub, T., and Wolchok, J.D. (2018). PD-L1 in tumor microenvironment mediates resistance to oncolytic immunotherapy. J. Clin. Invest. *128*, 5184.

27. Engeland, C.E., Grossardt, C., Veinalde, R., Bossow, S., Lutz, D., Kaufmann, J.K., Shevchenko, I., Umansky, V., Nettelbeck, D.M., Weichert, W., et al. (2014). CTLA-4 and PD-L1 checkpoint blockade enhances oncolytic measles virus therapy. Mol. Ther. *22*, 1949–1959.

28. Long, A.H., Haso, W.M., Shern, J.F., Wanhainen, K.M., Murgai, M., Ingaramo, M., Smith, J.P., Walker, A.J., Kohler, M.E., Venkateshwara, V.R., et al. (2015). 4-1BB costimulation ameliorates T cell exhaustion induced by tonic signaling of chimeric antigen receptors. Nat. Med. *21*, 581–590.

29. Wölfl, M., Kuball, J., Eyrich, M., Schlegel, P.G., and Greenberg, P.D. (2008). Use of CD137 to study the full repertoire of CD8+ T cells without the need to know epitope specificities. Cytometry A *73*, 1043–1049.

30. Eriksson, E., Milenova, I., Wenthe, J., Stahle, M., Leja-Jarblad, J., Ullenhag, G., Dimberg, A., Moreno, R., Alemany, R., and Loskog, A. (2017). Shaping the tumor stroma and sparking immune activation by CD40 and 4-1BB signaling induced by an armed oncolytic virus. Clin. Cancer Res. *23*, 5846–5857.

31. Jiang, H., Rivera-Molina, Y., Gomez-Manzano, C., Clise-Dwyer, K., Bover, L., Vence, L.M., Yuan, Y., Lang, F.F., Toniatti, C., Hossain, M.B., and Fueyo, J. (2017). Oncolytic Adenovirus and Tumor-Targeting Immune Modulatory Therapy Improve Autologous Cancer Vaccination. Cancer Res. *77*, 3894–3907.

32. Liu, K. (2010). Role of apoptosis resistance in immune evasion and metastasis of colorectal cancer. World J. Gastrointest. Oncol. *2*, 399–406.

33. Offner, S., Hofmeister, R., Romaniuk, A., Kufer, P., and Baeuerle, P.A. (2006). Induction of regular cytolytic T cell synapses by bispecific single-chain antibody constructs on MHC class I-negative tumor cells. Mol. Immunol. *43*, 763–771.

34. Zamarin, D., Holmgaard, R.B., Ricca, J., Plitt, T., Palese, P., Sharma, P., Merghoub, T., Wolchok, J.D., and Allison, J.P. (2017). Intratumoral modulation of the inducible co-stimulator ICOS by recombinant oncolytic virus promotes systemic anti-tumour immunity. Nat. Commun. *8*, 14340.

35. Zamarin, D., Holmgaard, R.B., Subudhi, S.K., Park, J.S., Mansour, M., Palese, P., Merghoub, T., Wolchok, J.D., and Allison, J.P. (2014). Localized oncolytic virotherapy overcomes systemic tumor resistance to immune checkpoint blockade immunotherapy. Sci. Transl. Med. *6*, 226ra32.

36. Rajani, K., Parrish, C., Kottke, T., Thompson, J., Zaidi, S., Ilett, L., Shim, K.G., Diaz, R.M., Pandha, H., Harrington, K., et al. (2016). Combination therapy with reovirus and anti-pd-1 blockade controls tumor growth through innate and adaptive immune responses. Mol. Ther. *24*, 166–174.

37. Bartlett, D.L., Liu, Z., Sathaiah, M., Ravindranathan, R., Guo, Z., He, Y., and Guo, Z.S. (2013). Oncolytic viruses as therapeutic cancer vaccines. Mol. Cancer *12*, 103.

38. Xu, D.P., Sauter, B.V., Huang, T.G., Meseck, M., Woo, S.L., and Chen, S.H. (2005). The systemic administration of Ig-4-1BB ligand in combination with IL-12 gene transfer eradicates hepatic colon carcinoma. Gene Ther. *12*, 1526–1533.

YMTHE, Volume *27*

Supplemental Information

Recombinant Adenovirus Expressing a Soluble Fusion Protein PD-1/CD137L Subverts the Suppression of $CD8^+$ T Cells in HCC

Yonghui Zhang, Hailin Zhang, Mei Wei, Tao Mou, Tao Shi, Yanyu Ma, Xinyu Cai, Yunzheng Li, Jie Dong, and Jiwu Wei

Supplementary figure 1

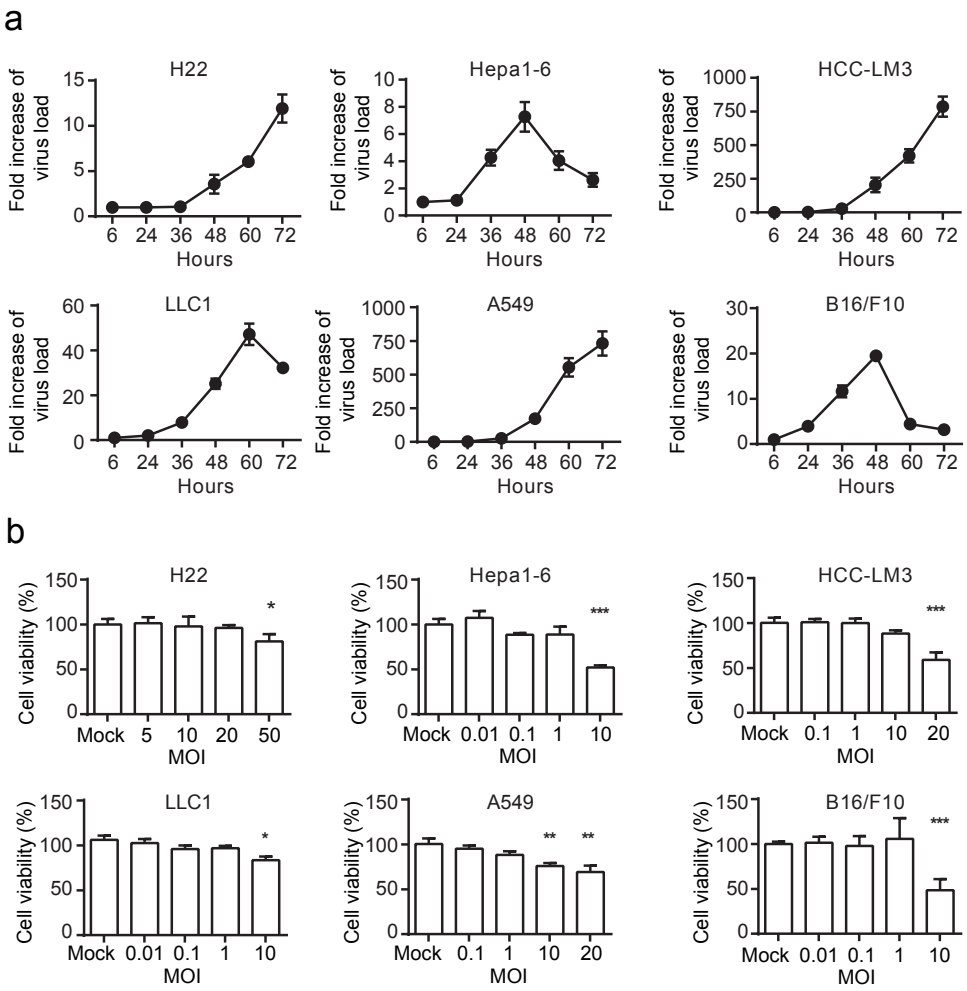

Figure S1 The capacity of Ad5con in replication and oncolysis.
a, H22, Hepa1-6, LM3, LLC, A549 and B16/F10 cells were infected with Ad5con at an MOI of 2 and were harvested at varying time points. DNA was extracted, and the viral copy number was determined by Q-PCR. The fold changes were calculated by dividing the copy number at 6 h. b, Cells were infected with Ad5con at the indicated MOI for 72 h, and the cell viability was determined by MTT. Data shown are means ± SD. * $p < 0.05$, ** $p < 0.01$, *** $p < 0.001$.

Table S1 Primers used in this study

Name	Sequences (5'-3')
GFP F	GACTCTAGAGGATCCGCCACCATGGTGAGCA
GFP R	TCTGCCCTCGCTAGCCTTGTACAGCTCGTCCAT
E1A F	ATCCCGGCCCTACCGGAATGAGACATATTATCTGCCAC
E1A R	AGCTTATCGATAGGTGTTATGGCCTGGGGCGTTTACAG
PD1 F	CCGCCACCATGACCGGTATGTGGGTCCGGCAG
PD1 R	GTGGTGGTGGTGGTGGTGGACCATGCCTTGAAACC
CD137L F	CAGGGGCCCTGGCTATGGCGCTCACAATCACCAC
CD137L R	GTGGTGGTGGTGGTGGTGTTCCCATGGGTTGTCG
CD33 F	CCGCCACCATGACCGGTATGCCGCTGCTGCTAC
PD1 R2	AACCGCCTCCACCGACCATGCCTTGAA
CD137L F2	CGGTGGCGGATCGGCGCTCACAATCACCAC
Q-E1A F	CCTTCTAACACACCTCCTGAGATACA
Q-E1A R	CAGGCTCGTTAAGCAAGTCCTC
GAPDH F	CAAGCAATCACCTCTTGGACAGGA
GAPDH R	CCCACCCTAGAAAGTCCAAAGAGATC